International Journal of Research in Economics and Social Sciences(IJRESS)
Available online at: http://euroasiapub.org
Vol. 14 Issue 1, Jan- 2024
ISSN(o): 2249-7382 | Impact Factor: 8.018
(An open access scholarly, peer-reviewed, interdisciplinary, monthly, and fully refereed journal.)

Study on Spatially Controlled Atomic Layer Deposition in Porous Materials with Some of StableMaterials

[1]Anu Yadav, [2] Dr. Priyanka Mathur, [3] Dr. Anil Kumar Sharma

[1] Research Scholar, (Chemistry)

[2] Researches Guide, Dr. Priyanka Mathur, & Dr. Anil Kumar Sharma

Bhagwant, University, Ajmer, Raj. India

Email Id-yadavanu241@gmail.com

Phy. Research Paper-Accepted Dt. 14 Dec. 2023 **Published** : Dt. 15Jan. 2024

Abstract

The research paper introduces a novel method for depositing materials into porous surfaces with controlled depths, leveraging the passivating action of one precursor to hinder the adsorption of a second precursor. For instance, diethyl zinc does not react with a surface treated with trim ethyl aluminum. This property facilitates spatially controlled "stripe coating" within the deposited layer, facilitated by Knudsen diffusion that determines the depth of penetration based on precursor exposure lengths. By demonstrating ZnO stripes within permeable anodic alumina supports and employing Monte Carlo simulations for prediction, the study highlights the efficacy of the method. Additionally, it proposes a technique to apply chemicals at specified depths on porous surfaces by utilizing the passivating effect of one precursor to impede the adsorption of another. Despite its advantages, the method may encounter challenges, particularly with certain precursor combinations leading to etching. Etching refers to the dissolution or removal of material from a solid surface. In this context, it suggests that some precursor combinations may result in undesired erosion or alteration of the porous surface during the deposition process. Understanding and mitigating such issues are crucial for the method's practical application and broader utility in materials science and engineering contexts.

Keywords: Atomic layer deposition ALD, Anodic aluminum oxide AAO, diethyl zinc DEZ and 2D metals.

International Journal of Research in Economics and Social Sciences(IJRESS)
Available online at: http://euroasiapub.org
Vol. 14 Issue 1, Jan- 2024
ISSN(o): 2249-7382 | Impact Factor: 8.018
(An open access scholarly, peer-reviewed, interdisciplinary, monthly, and fully refereed journal.)

Introduction

Atomic Layer Deposition (ALD) stands out as a sophisticated thin-film growth technique that facilitates the controlled deposition of materials at the atomic level, ensuring precise layering on solid surfaces. ALD operates through alternating, self-limiting reactions between gaseous precursors and a substrate, enabling the creation of highly conformal and uniform films even on complex, three-dimensional substrates such as aerogels, powders, and anodic aluminum oxide (AAO) membranes. The use of ALD on porous substrates is particularly intriguing as it opens avenues for creating nanostructured catalysts with enhanced functionalities. Traditionally, ALD has been applied extensively to penetrate porous substrates, resulting in uniform coatings on all interior surfaces. However, there's growing interest in confining catalytic activity to specific, controlled regions of porous substrates, which offers distinct advantages. For instance, organizing catalytic materials into "stripes" along nonporous walls in a predetermined order can optimize catalytic performance and facilitate specific chemical reactions. Until now, achieving patterned ALD on porous substrates has been a challenge, mainly because of the inherent complexity of such substrates. However, the method described in the research paper presents a novel approach to achieve controlled ALD patterning on porous substrates. The key lies in leveraging the passivating effect of one ALD precursor to prevent the application of a second precursor during subsequent exposures, thus enabling precise control over where materials are deposited within the porous structure.

To illustrate, consider the process involving trim ethyl aluminum (TMA) and diethyl zinc (DEZ) as ALD precursors. Initially, when a hydroxylated surface is exposed to trim ethyl aluminum (TMA), it becomes passivated, rendering it unreactive to subsequent exposure to aluminum TMA. This passivation effect creates a controlled environment where only specific regions of the substrate remain reactive to subsequent precursors like diethyl zinc (DEZ). By manipulating precursor exposures and employing Knudsen diffusion, materials can be distributed within the porous structure in a controlled manner. Knudsen diffusion plays a crucial role in this process by ensuring that reactive sites within the porous substrate

International Journal of Research in Economics and Social Sciences(IJRESS)
Available online at: http://euroasiapub.org
Vol. 14 Issue 1, Jan- 2024
ISSN(o): 2249-7382 | Impact Factor: 8.018
(An open access scholarly, peer-reviewed, interdisciplinary, monthly, and fully refereed journal.)

are filled in a sequential manner, typically starting from the pore entrances. By utilizing sub-saturating TMA exposure, it's possible to ensure that the pore entry regions are reacted with TMA first, providing a foundation for subsequent material deposition. This controlled approach allows for the precise patterning of catalytic materials within the porous substrate, offering unprecedented control over catalytic activity and selectivity. The implications of this method are significant, particularly in the realm of catalysis and materials science. By confining catalytic activity to specific regions within porous substrates, researchers can design catalysts with tailored functionalities for various applications, including chemical synthesis, environmental remediation, and energy conversion. Furthermore, the ability to achieve controlled ALD patterning on porous substrates opens up new possibilities for designing advanced materials with enhanced performance and functionality.

Anodic aluminum oxide AAO

The AAO membranes utilized in this process possess specific dimensions, featuring a pore width of 56 nm and a thickness of 75 μm, as established through meticulous preparation methods. To maintain a gastight connection with face-seal fittings, an aluminum ring encircling the AAO membrane was preserved using a masking procedure, ensuring a controlled environment for the subsequent ALD processes.

In order to facilitate precise deposition, the membranes were positioned within a specially designed apparatus. This device ensures that the precursor gases only interact with one side of the membrane during the coating process, preventing unintended reactions and ensuring uniformity in deposition.

Within a bespoke viscous flow reactor, (ZnO)and Al_2O_3 were synthesized through alternating exposures of diethyl zinc (DEZ) with water vapor (H2O) and trimethyl aluminum (TMA) with water vapor (H2O) at a temperature of 150°C. This controlled environment promotes the self-limiting reactions characteristic of ALD, enabling atomic layer deposition of materials onto the membrane surface.

For the creation of titanium dioxide (TiO2) and vanadium pentoxide (V2O5), vanadium oxytriisopropoxide with hydrogen peroxide (H2O2) and titanium tetrachloride with hydrogen peroxide (H2O2) were utilized, respectively.

International Journal of Research in Economics and Social Sciences(IJRESS)
Available online at: http://euroasiapub.org
Vol. 14 Issue 1, Jan- 2024
ISSN(o): 2249-7382 | Impact Factor: 8.018
(An open access scholarly, peer-reviewed, interdisciplinary, monthly, and fully refereed journal.)

The ALD timing sequences, denoted as *t1-t2-t3-t4-t5-t6*, adhere to a structured protocol:

- t1, t3, and t5 represent the exposure times for the first, second, and third precursors, respectively, measured in seconds.
- t2, t4, and t6 denote the corresponding purge times after the exposures, also measured in seconds.

These timing sequences ensure the controlled and sequential deposition of precursor gases onto the membrane surface, promoting the formation of uniform and conformal thin films.Overall, the experimental setup involving AAO membranes, the meticulously controlled ALD processes, and the timing sequences employed underscore the precision and reproducibility of the deposition technique, showcasing its potential for applications in various fields such as catalysis, sensing, and nanotechnology.

2D Metals

The realm of two-dimensional (2D) materials extends beyond graphene and encompasses a variety of stable structures found in oxides, hexagonal boron nitride (h-BN), and Transition Metal Dichalcogenides (TMDs) such as MX2, where X = S, Se, or Te, and M = Mo or W. These materials are characterized by their layered crystalline structure, held together by Van der Waals (VdW) forces, allowing for easy exfoliation into one or more layers.

The high surface-to-volume ratio inherent in 2D materials significantly impacts their mechanical and chemical properties, electronic confinement, and optical and electronic properties due to their reduced dimensions. This unique set of characteristics positions 2D materials as highly promising candidates in cutting-edge fields such as gas sensing, renewable energy, catalysis, micro- and opt-electronics, and environmental applications.

While considerable attention has been directed towards the synthesis and applications of 2D materials using techniques like Atomic Layer Deposition (ALD), there remains a need for comprehensive reviews of recent developments in the field. Despite the abundance of publications detailing the use of ALD for creating 2D materials, the focus on the most well-known materials has been relatively scant.

International Journal of Research in Economics and Social Sciences(IJRESS)
Available online at: http://euroasiapub.org
Vol. 14 Issue 1, Jan- 2024
ISSN(o): 2249-7382 | Impact Factor: 8.018
(An open access scholarly, peer-reviewed, interdisciplinary, monthly, and fully refereed journal.)

It's worth noting that the family of 2D materials under ambient conditions encompasses stable, potentially stable, and unstable materials, some of which are still theoretical in nature. This diversity underscores the richness and complexity of the 2D materials landscape and highlights the importance of continued research and exploration in this area.

As researchers delve deeper into the synthesis, characterization, and applications of 2D materials, a deeper understanding of their properties and behaviors emerges, paving the way for innovative advancements in various technological and scientific domains. Additionally, comprehensive reviews of recent developments in ALD of sulfides and dichalcogenides contribute to the collective knowledge base, guiding future research directions and facilitating the realization of the full potential of 2D materials in diverse applications.

Results and Conclusion

The Zn L_ EDAX maps versus the TMA exposure period are displayed in Figure 1. With longer TMA exposure durations, the Zn signal narrows and shifts to greater distances. It looks like a stripe. Since ZnO does not deposit on the outside AAO pores exposed to the TMA, it is evident that the TMA functions as an efficient mask for the subsequent ZnO development. In the past, masking agents for selective ZnO ALD have included self-assembled monolayers, or _SAMs_, comprising long-chained, hydrophobic alkenes such docosyltrichlorosilaneDTS.SixBut the DTS SAM is limited to

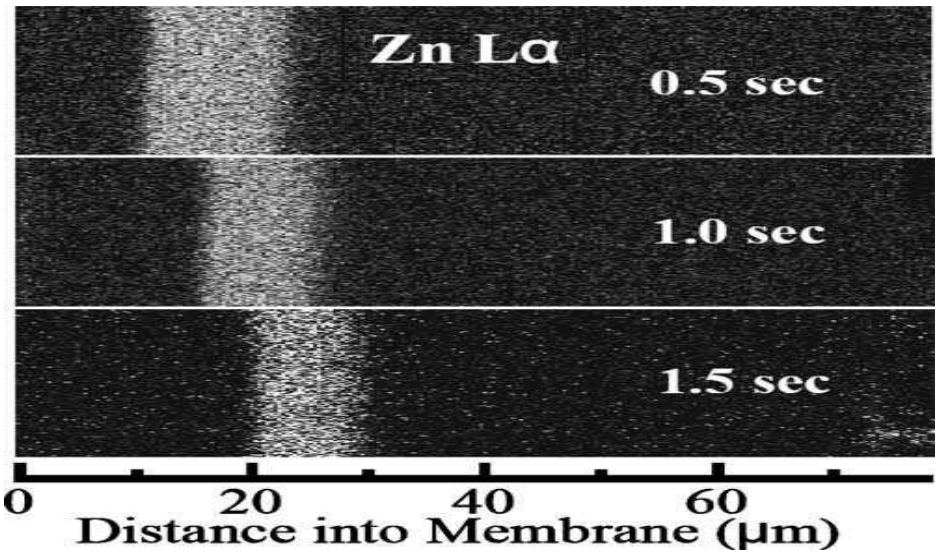

FIG. 1. EDAX elemental maps for Zn *L*_ following deposition of ZnOstripes in AAO varying only the TMA exposure time.

International Journal of Research in Economics and Social Sciences(IJRESS)
Available online at: http://euroasiapub.org
Vol. 14 Issue 1, Jan- 2024
ISSN(o): 2249-7382 | Impact Factor: 8.018
(An open access scholarly, peer-reviewed, interdisciplinary, monthly, and fully refereed journal.)

whereas our technology makes it possible to do selective ZnO ALD on three-dimensional objects at the same time. be conceived of on a surface that is level. Integrated line scans were produced by integrating the EDAX images shown in Figure 1 along the lateral dimension that is perpendicular to the AAO pores. These line scans are displayed in Figure 2a. The outcomes of the ZnO stripe coating trials are depicted in Figure 2b. These experiments were carried out with Monte Carlo simulations8 and utilized the same timing sequences as Figure 2a. In these simulations, the pores of the AAO were modeled as a one-dimensional array, and the movements of individual molecules of TMA and DEZ were tracked.

An approximation of Knudsen diffusion was achieved by employing a one-dimensional random walk with a hop length that was similar to the diameter of the local pores. A chemical reaction on an empty site is possible after each hop, and the probability of such a reaction occurring is equal to the reactive sticking coefficient. The molecule continued along each pathway until it either exited the tube or interacted with something else.

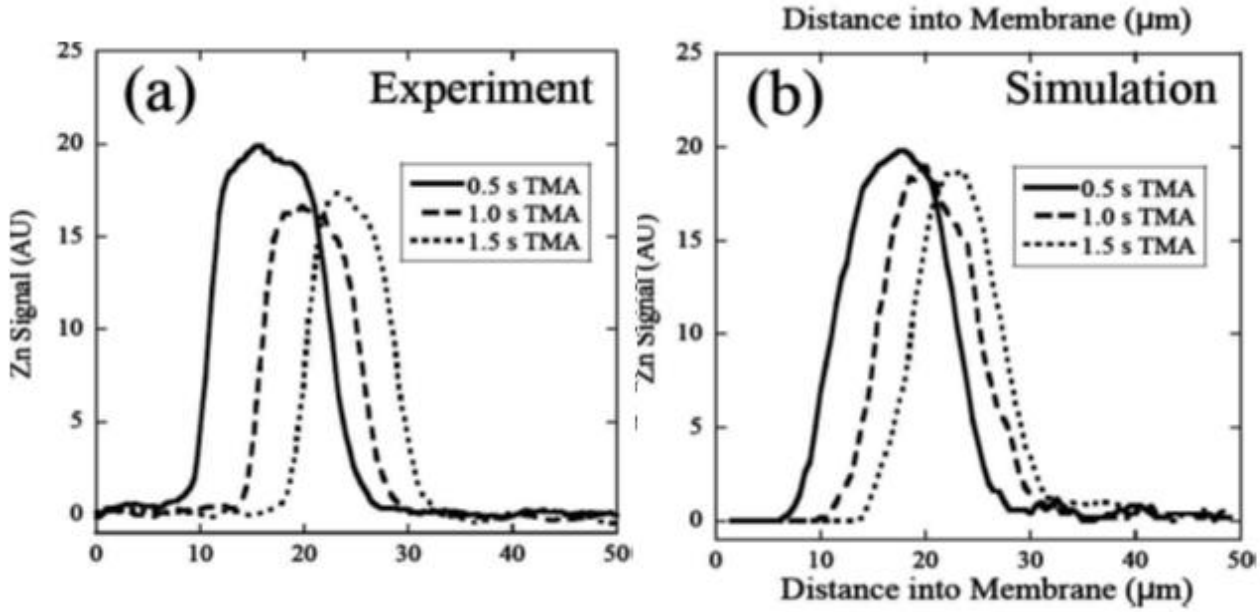

FIG. 2. Zn L line scans, both simulated and experimental, for ZnO stripes in AAO that match the elemental maps in Figure 1. As shown in Fig. 3, with surface hydroxyl groups and deposit Zn between the stripes. Zn etching by TMA has been documented in the past. The reason for this behavior could be that ZnO has a formation enthalpy of −353 kJ/mol Zn atoms, while Al2O3 has a formation enthalpy of −845 kJ/mol Al atoms.

International Journal of Research in Economics and Social Sciences(IJRESS)
Available online at: http://euroasiapub.org
Vol. 14 Issue 1, Jan- 2024
ISSN(o): 2249-7382 | Impact Factor: 8.018
(An open access scholarly, peer-reviewed, interdisciplinary, monthly, and fully refereed journal.)

This result shows that certain combinations of precursors are not appropriate for ALD stripe coating. ZnO, TiO2, and V2O5 stripes were created inside AAO membranes at specific depth positions by using TMA as a masking agent. We presume that this approach is generic and that masking agents might be derived from various precursors. We also used spherical silica gel particles and other nanoporous supports using this approach. This method will make it possible to create nanoporous membranes for sequential catalysis reactions.

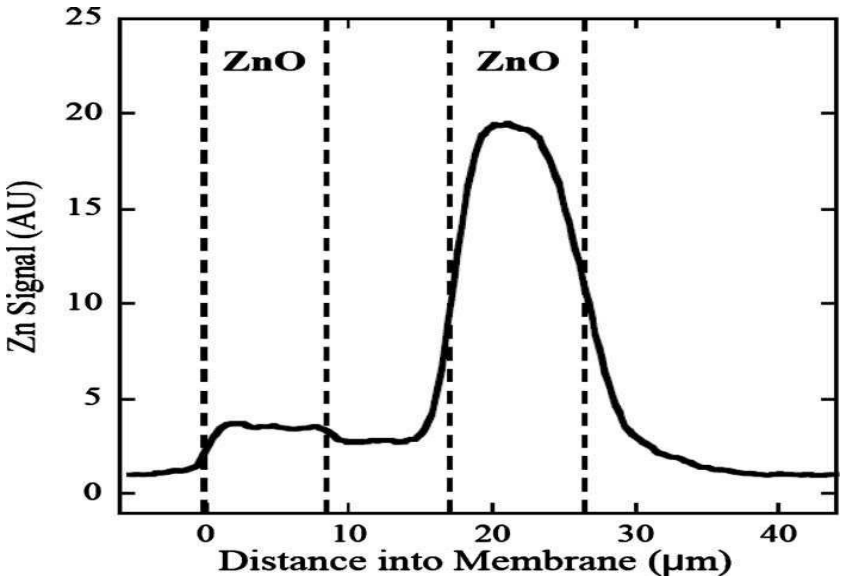

FIG. 3. Zn *L*_ line scan following attempted two-stripe ZnO coating inAAO. Dashed lines indicate expected locations of Zn stripes.

Fabrication of other layered chalcogenides

ALD has also been used to create a variety of metal chalcogenides, including metal sulfides, in addition to Mo and W TMDs. There are presently around 300 publications in the literature, many of which were written before the grapheme isolation. But the majority of materials deposited by ALD are not two-dimensional layered structures. In fact, "only SnSx (x = 1 or 2), 88,133–144 GeS, 88 γ-MnS, 89 TiS2,145,146 GaS, 90,147 γ-InSe, 93 Bi2Te3,148–152 Bi2Se3,153 Bi2S3,154 Sb2Te3,148 Sb2Se3 93", and the less well-known β- NiS91 and FeSx,92 exhibit layered rhombohedral, orthorhombic, or hexagonal crystalline phase and are likely stable 2D materials.4, 5, 17, 38, 39 A brief overview of the precursors and ALD techniques utilized to create these 2D materials will be provided below. The primary ALD conditions and potential uses for each 2D material are presented in Table 1.

International Journal of Research in Economics and Social Sciences(IJRESS)
Available online at: http://euroasiapub.org
Vol. 14 Issue 1, Jan- 2024
ISSN(o): 2249-7382 | Impact Factor: 8.018
(An open access scholarly, peer-reviewed, interdisciplinary, monthly, and fully refereed journal.)

At 390°C, WS2 and SnS are alternately annealed (ALD) to effectively create WS2/SnS 2D heterostructures on SiO2/Si. The stacking of the two layered materials is demonstrated by the HRTEM examination, as seen in Figure 5c,d. Due of the lattice mismatch caused by their distinct crystal structures, a 15° angle is seen between their c axes.

The hole mobility of SnS is significantly reduced as a result of this misalignment, which was determined by the utilization of back-gated transistor devices. Because of this, two-dimensional heterostructures appear to have a greater potential for electrical applications when they have a crystalline structure that is comparable.

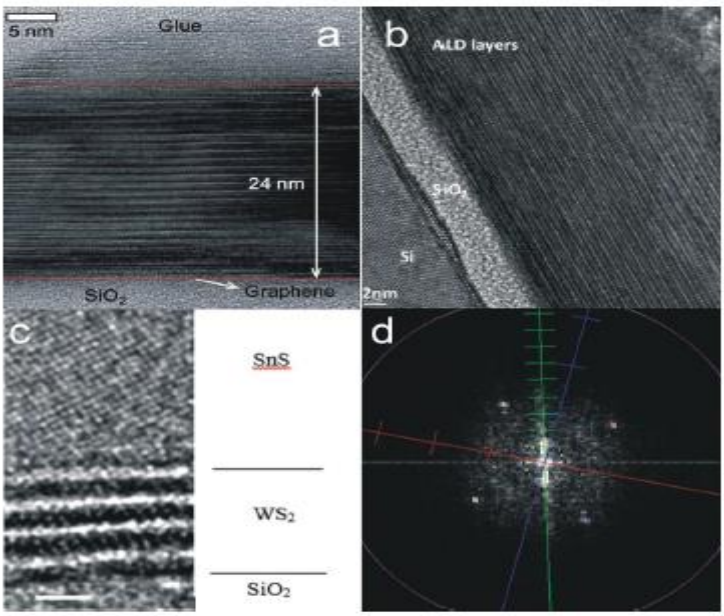

Figure 5. a) A figure showing a cross-sectional HRTEM image of a Sb2Te3 film that was grown on graphene/SiO2. The reference has granted permission for this reproduction. b) A cross-sectional image obtained from a HRTEM demonstrating the stack of ALD Sb2Te3/Bi2Te3 layers supported by SiO2. This is a reproduction of reference 157, with permission. c) The HRTEM image of the contact between SnS and WS2 in relation to the cross-section, and d) the FFT associated with the image. There is one nanometer represented by a scale marker. At the same time that the interlayer spacing of WS2 is depicted in green, the c* and b* axes of SnS are depicted in blue and red, respectively. The reference has granted permission for this reproduction.

International Journal of Research in Economics and Social Sciences(IJRESS)
Available online at: http://euroasiapub.org
Vol. 14 Issue 1, Jan- 2024
ISSN(o): 2249-7382 | Impact Factor: 8.018
(An open access scholarly, peer-reviewed, interdisciplinary, monthly, and fully refereed journal.)

Table 1. This article provides an overview of the applications of the published ALD techniques on metal dichalcogenides, including those that are stable and those that are predicted to be stable. QCM is an abbreviation for the quartz crystal that is used for QCM, T is an abbreviation for the temperature at which the deposition is taking place, SiO2/Si is an abbreviation for SiO2 coated Si, (SW)CNT and CFP are abbreviations for (single-walled) carbon nanotubes and carbon fiber paper, respectively, and ITO (FTO) is an abbreviation for indium tin oxide, which is fluorine doped tin oxide. Note that the ALD window is highlighted.

Material	Technique	Reactants	Substrate	Operating temperature	Post-treatment	Crystallinity	Application
MoS_2	SLS	$MoCl_5/H_2S$	SiO_2/Si, WSe_2 flakes	500 °C (3L), 700 °C (2L), 900 °C (1L)	None	polycrystalline	FET, p-n diode
	ALD		Al_2O_3(0001)	300 °C	800 °C for 30 min in S atm	Well-crystallized, hexagonal	-
			SiO_2/Si	330-450 °C	None	Well-crystallized, hexagonal	FET
			300 nm SiO_2/Si(100)	450	None	Well-crystallized, hexagonal	FET
			Si, Al_2O_3	420-490	None	Nanocrystalline, size function of T 430 °C≤T≥470 °C: h-MoS_2 (0002) orientated	-
			SiO_2/Si (patterned), quartz	375, 475 °C	600-900 °C for 30 min in either S atm or H_2S	Small crystallites with basal planes having preferential orientation // substrate	-
		$Mo(thd)_3/H_2S$	SiO_2/Si, soda lime glass, ALD Al_2O_3, ALD Ir, ALD SnS, Si-H, sapphire, ITO-coated glass, ALD ZnS, ALD SnO_2, borosilicate	250-350 °C	None	Crystallinity function of the support	-
		$Mo(NMe_2)_4/H_2S$	QCM, amorphous Al_2O_3, photoresist/Si_3N_4	60-120 °C	1000 °C for 5h under S atm	Polycrystalline preferential orientation	-
		$Mo(NMe_2)_4/HS(CH_2)_2SH$	SiO_2/Si, SiO_2 particles	50 °C	450 °C for 30 min in H_2 Or 800 °C for 30 min in Ar	In H_2: Nanocrystalline In Ar: Well-crystallized	-
		$Mo(CO)_6/CH_3S_2CH_3$	SiO_2/Si	100 °C	None 900 °C for 30 min in Ar	A deposited: Amorphous Annealed: Crystalline (002) orientation	-
			Au/Ti/Si	100 °C	None	Amorphous	HER
			CFP, Si	-	None	Mix amorphous nanocrystallites	HER
		$Mo(CO)_6/H_2S$	QCM, SiO_2/Si, KBr pellets, glass slide, stainless steel	155-170 °C	None	Amorphous	Li ion battery
			SiO_2/Si	155-175 °C*	RTA at 900 °C in either H_2S or Ar	As-grown amorphous Annealed: well-crystallized with preferential (002) orientation // substrate	-
			Co porous foam	200 °C	None	nanocrystals	OER

International Journal of Research in Economics and Social Sciences(IJRESS)
Available online at: http://euroasiapub.org
Vol. 14 Issue 1, Jan- 2024
ISSN(o): 2249-7382 | Impact Factor: 8.018
(An open access scholarly, peer-reviewed, interdisciplinary, monthly, and fully refereed journal.)

	PEALD	$Mo(CO)_6/H_2S$ plasma	SiO_2/Si, GaN, Sapphire	175-225 °C (175-200 °C*)	None	polycrystalline 2H-MoS_2	-
			p-Si photocathode	200 °C	500-700 °C in H_2S	polycrystalline	Photoectrochemical water reduction HER
	ALD MoO_3	$Mo(CO)_6$/ozone	SiO_2/Si, glassy carbon, CFP	165 °C	Sulfurization S atm	polycrystalline randomly oriented	HER
			SiO_2/Si Sapphire	165 °C	Sulfurization S atm	Cluster Down to 2L of h-MoS_2	-
		$(N^tBu)_2(NMe_2)_2Mo/O_3$	SiO_2/Si	300 °C	Sulfurization H_2S	Function of the process 2H-phase	-
	PEALD MoO_3	$Mo(CO)_6/O_2$ plasma	SiO_2/Si	200 °C	2 step sulfurization	Polycrystalline	-
		$(N^tBu)_2(NMe_2)_2Mo/O_2$ plama	SiO_2/Si	150 °C	Sulfurization H_2S	Function of the process 2H-phase	-
	ALET	Cl radical ads/ Ar, desorp	CVD MoS_2 on SiO_2/Si	-	None	2H-MoS_2, well crystallized	-
			exfoliated MoS_2	-	None	2H-MoS_2, well crystallized	FET
			CVD MoS_2 on sapphire, SiO_2	20 °C	None	2H-MoS_2, well crystallized	-
		O_2 plasma/Δ 500 °C	exfoliated MoS_2	200 °C	None	2H-MoS_2, well crystallized	-
Nb:$MoSe_2$	PEALD Nb_2O_5	-	Evaporated MoO_3	-	Selenization	Polycrystalline	Gas sensing
$Mo_{1-x}W_xS_2$	PEALD $Mo_{1-x}W_xO_y$	$Mo(CO)_6/O_2$ plasma $WH_2(^iPrCp)_2/O_2$ plasma	SiO_2/Si	200 °C 300 °C	2 step sulfurization	Alloy with honeycomb lattice – vertically composition control	photodetector
WS_2	PEALD	WF_6/H_2 plasma/H_2S	Amorphous and polycrystalline Al_2O_3/Si(100)	300-450 °C	None	Nanocrystalline T=300 °C: preferential (0002) orientation T=450 °C: random orientation	-
	ALD	WF_6/H_2S + Zn catalyst (DEZ or ZnS layer)	SiO_2/Si, Au, MEMS	250-350 °C	None 500 °C for 1h in vacuum	h-(002) texture no change when annealed	Solid lubricant
		WF_6/H_2S + Si layer catalyst	Al_2O_3/Si(100)	300-450 °C	None	Nanocrystalline, orientation depending on T	-
		WCl_6/H_2S	SiO_2/Si(100)	390 °C	None	2H-phase	back-gated transistor 2D-heterostructure
		$W(CO)_6/H_2S$	SiO_2/Si(100), ZnS/SiO_2/Si(100)	400 °C	None	Hexagonal (002) (101) orientation	Solid lubricant
			Si(111), microscope glass, stainless steel, CNTs	175-205 °C*	None	Amorphous	Li-ion battery
	PEALD WO3	$WH_2(^iPrCp)_2/O_2$ plasma	SiO_2/Si (wafer+nanowires)	300 °C	Sulfurization Ar/H_2S	hexagonal	FET Gas sensor
Al :WS_2	PEALD Al :WO_3	$W(NMe_2)_4(N^tBu)_2/O_2$ plasma/TMA	quartz	150 °C	Sulfurization CS_4	2H-WS_2 (002) orientation Doping reduces crystallinity	-
WSe_2	ALD	WCl_6/H_2S	SiO_2/Si	390 °C	None	Well-crystallized, hexagonal	FET
	SLS	WCl_6/DESe	SiO_2/Si	600 °C (5L), 700 °C (3L), 800 °C (1L)	None	Well-crystallized, hexagonal	FET

Conclusion

The creation of catalysts for environmental protection was the goal of this endeavor. The catalyst deposition of TiO2 by ALD in conjunction with DBD for toluene breakdown and the catalyst deposition of CeO2, Ag2O, and Ag-doped CeO2 by ALD for diesel soot combustion were the main points of interest. The following conclusions can be made in light of the findings covered in this thesis and the articles that are appended: On planar silicon substrates, the nucleation regime and development of TiO2 thin films produced by ALD at 350 °C were investigated. The findings demonstrated that 80 cycles are needed for silicon that has been plasma treated, while 50 cycles are needed to begin producing a continuous TiO2 coating on untreated silicon substrates. The size of individual crystallites generated on silicon can be evaluated using the quantum confinement impact on optical band gap; the obtained results are consistent with AFM measurements.

International Journal of Research in Economics and Social Sciences(IJRESS)
Available online at: http://euroasiapub.org
Vol. 14 Issue 1, Jan- 2024
ISSN(o): 2249-7382 | Impact Factor: 8.018
(An open access scholarly, peer-reviewed, interdisciplinary, monthly, and fully refereed journal.)

References

1. Novoselov, K. S. et al. Electric field effect in atomically thin carbon films. Science 306, 666–669 (2004).
2. Mas-Ballesté, R., Gómez-Navarro, C., Gómez-Herrero, J. & Zamora, F. 2D materials: to grapheme and beyond. Nanoscale 3, 20–30 (2011).
3. Butler, S. Z. et al. Progress, Challenges, and Opportunities in Two-Dimensional Materials
4. Beyond Graphene. ACS NANO 7, 2898–2926 (2013).
5. Choi, W. et al. Recent development of two-dimensional transition metal dichalcogenides and
6. their applications. Mater. Today (2017).
7. Xu, M., Liang, T., Shi, M. & Chen, H. Graphene-Like Two-Dimensional Materials. Chem. Rev. 113, 3766–3798 (2013).
8. Liu, Y. et al. Van der Waals heterostructures and devices. Nat. Rev. Mater. 1, 16042 (2016).
9. Irani, R., Naseri, N. & Beke, S. A review of 2D-based counter electrodes applied in solar-assisted devices. Coord. Chem. Rev. 324, 54–81 (2016).
10. Hu Yun Hang, Wang Hui & Hu Bo. Thinnest Two-Dimensional Nanomaterial—Graphene forSolar Energy. ChemSusChem 3, 782–796 (2010).
11. Sun, Z., Ma, T., Tao, H., Fan, Q. & Han, B. Fundamentals and Challenges of Electrochemical CO2 Reduction Using Two-Dimensional Materials. CHEM 3, 560–587 (2017).
12. Kumar, A. & Xu, Q. Two-Dimensional Layered Materials as Catalyst Supports. CHEMNANOMAT 4, 28–40 (2018).
13. M. Ritala and M. Leskela, in Handbook of Thin Film Materials, edited byH. S. Nalwa _Academic, San Diego, 2001_, Vol. 1, p. 103.
14. M. J. Pellin, P. C. Stair, G. Xiong, J. W. Elam, J. Birrell, L. Curtiss, S. M.
15. George, C. Y. Han, L. Iton, H. Kung, M. Kung, and H. H. Wang, Catal.Lett. 102, 127 _2005.